

Electrostatic interactions in a neutral model phospholipid bilayer by molecular dynamics simulations

Leonor Saiz^{a)} and Michael L. Klein

Center for Molecular Modeling and Chemistry Department, University of Pennsylvania, Philadelphia, Pennsylvania 19104-6323

(Received 29 March 2001; accepted 27 November 2001)

The organization of the lipid headgroups in a neutral model membrane is studied by atomistic simulations in the fluid lamellar phase, L_α . In particular, we report the results obtained for a fully hydrated 1-stearoyl-2-docosahexaenoyl-*sn*-glycero-3-phosphocholine lipid bilayer at room temperature. The orientational distribution of the lipid dipole moments with respect to the membrane normal presents a maximum at 70° (20° above the plane of the interface, pointing toward the water region). We also found another smaller peak at 110° (-20° with respect to the membrane plane). This preferential orientation of the lipid headgroup dipoles with respect to the bilayer normal obtained at 303 K is qualitatively different from previous calculations at higher temperatures in the fluid lamellar phase, where headgroup dipoles were uniformly distributed with orientations spanning 0° – 135° . Despite their differences, both situations give rise to a similar mean orientation of $\sim 70^\circ$, which is in excellent agreement with experiment. The statistics of the main lipid–lipid interactions, the charge density profiles, the electrostatic potential along the bilayer normal, and the polarization of water molecules at the interfacial plane are also analyzed. © 2002 American Institute of Physics. [DOI: 10.1063/1.1436077]

I. INTRODUCTION

Lipids are the main component and the structural basis of biomembranes, which separate the living cells and their organelles from the environment. These amphiphilic molecules in water also display a rich variety of mesophases, which are controlled mainly by temperature and lipid/water composition.¹ Among these structures, the fluid lamellar phase, L_α , is the most relevant in biological membranes.

Phospholipids, the major class of membrane lipids, have two hydrophobic acyl chains and different hydrophilic headgroups, either charged or neutral. Even in phospholipid bilayers with neutral headgroups, the electrostatic interactions constitute a basic ingredient in the structural properties of membranes. Electrostatics also plays a fundamental role in the interactions among membranes or vesicles, membranes and other objects of biological interest, and membranes with external fields. Membrane permeation, insertion of proteins or peptides in membranes, DNA-lipid complexes (see Ref. 2 for a recent review), fusion of vesicles and membranes, and electroporation, just to mention a few processes, are governed primarily by electrostatic interactions.¹

In the case of neutral phosphatidyl choline (PC) lipids, charges are arranged in a way that there is a net headgroup dipole, within the range 18.5–25 D.³ The phosphate group, which is linked to the glycerol backbone, has a net negative charge, while the choline group, which constitutes the free end of the headgroup, has a net positive charge. In fully hydrated membranes in the L_α phase, the lipid headgroups form a network of interacting moieties to minimize the electrostatic interactions at the lipid-water interface,^{4,5} the most

polar region of the membrane. In this network, water molecules interact with the lipid headgroups and even form bridges among them. The microscopic origin of the membrane surface charge and dipole distribution is thus the organization at the interface of the polar headgroups and the counteracting effect of the polarized hydrating water molecules. The latter also constitutes the most likely origin of the hydration forces between membrane surfaces.¹ Due to the slow diffusive motion of the lipid headgroups compared to the water molecules, the main structure is driven by the former, whereas the latter rearrange themselves in order to neutralize the effect of the lipids at the interface. Headgroup dipole correlations in the interfacial plane fade away after a few molecular diameters and, on average, there is a null net dipole arising from the lipids in the interfacial plane.⁴

The situation is different when one considers the component of the headgroup dipole in the direction of the bilayer normal, which is perpendicular to the lipid-water interface. Experimentally, mainly from NMR and x-ray measurements, it was obtained that, in neutral membranes, there is a net component of the electrostatic dipole along the bilayer normal. On average, the headgroup dipoles lie approximately parallel, within 30° , to the membrane plane.^{3,6,7} Similar characteristics have been obtained for phospholipids with phosphatidyl glycerol (PGs) headgroups and with different neutral headgroups, such as PCs and phosphatidyl ethanolamines (PEs), for temperatures well into the L_α phase.⁶ Hence, this behavior has been considered as a common feature of the lipid headgroup dipoles in the L_α phase.

In this article, we analyze the organization of the lipid headgroup dipoles at the membrane interface in the fluid lamellar phase, L_α , at room temperature. We also study the

^{a)}Electronic mail: leonor@cmm.chem.upenn.edu

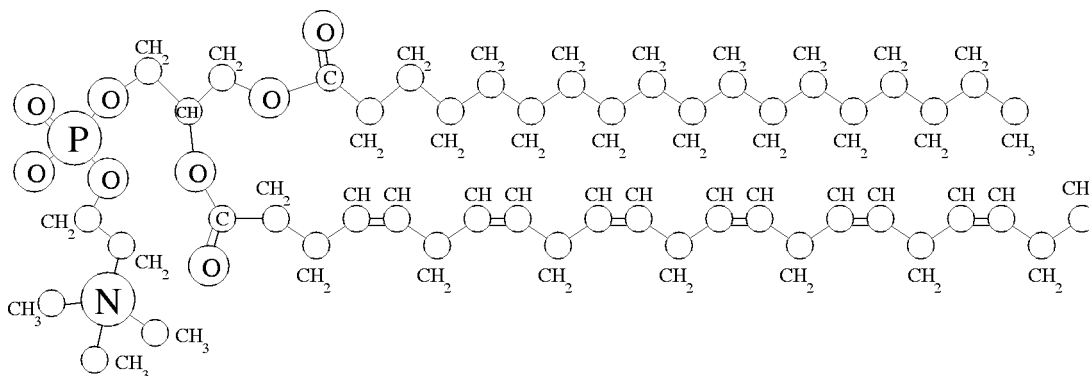


FIG. 1. Schematic representation of the molecular structure of SDPC. The single and double covalent bonds of the two fatty acid units and the headgroup are shown as single and double lines, respectively. For the sake of clarity, the hydrogen atoms are not explicitly shown in the sketch, even though in the MD simulations all the atoms were considered as individual interaction sites.

counteracting effect of the water molecules hydrating the lipid headgroups and their contribution to the total electrostatic potential across the membrane interface. Our results are based on a model membrane, which consisted of a fully hydrated lipid bilayer. Specifically, we chose a mixed (polyunsaturated/saturated) chain lipid, the so-called 1-stearoyl-2-docosahexaenoyl-*sn*-glycero-3-phosphocholine (SDPC). For this system, the main order–disorder phase transition between the biologically relevant fluid lamellar phase and the more ordered gel phase ($L_{\beta'}$) occurs at a temperature, T_m , of approximately -5°C .⁸ The fluid lamellar phase is characterized by liquidlike chains, whereas, in the gel phase, the chains are essentially adopting an all-*trans* conformation but less tightly packed than in a crystal and tilted to accommodate the packing mismatch between lipid headgroups and lipid chains. On the one hand, this low T_m temperature allows us to address the membrane electrostatics at room temperature while remaining well into the fluid lamellar phase, since the presence of the polyunsaturated chains increase the disorder of the membrane interior and, due to their different conformation, hinder the lateral packing of the lipid chains. On the other hand, the components of this type of membrane have some interesting properties and are quite abundant in the tissues of the retina, brain, and olfactory bulb.⁹ In particular, multiple unsaturations (double-bonds) affect a number of the membrane biophysical properties^{4,10} and, specifically, the docosahexaenoic fatty acid (DHA) content is known to modify the activity^{11–13} of the visual receptor rhodopsin.¹⁴ We use classical molecular dynamics (MD) simulations to explore this organization at the microscopic level.

II. SIMULATION SYSTEM AND METHODOLOGY

The studied model membrane represents a fully hydrated SDPC lipid bilayer, which was constituted by 64 lipid molecules (32 per monolayer) and about 27.5 water molecules per lipid. The SDPC lipid consists of a neutral (PC) headgroup, a long saturated chain with 18 carbon atoms, and a polyunsaturated chain with 22 carbon atoms and six *cis* double bonds. In Fig. 1, we show a sketch of the SDPC molecule where the hydrogen atoms are not explicitly drawn. The system was examined by performing classical MD simu-

lations at constant temperature, $T=303\text{ K}$, and pressure, $P=1\text{ atm}$, with similar characteristics to those reported previously.⁴ Following the standard procedures, the simulations consisted of an equilibration period (almost 2 ns) and an equilibrium period of 1 ns at constant pressure, number of molecules, and temperature (NPT ensemble) with a flexible orthorhombic simulation cell. During the equilibrium period, we computed the different properties and the dimensions of the lipid bilayer were characterized by $A=61.4\pm 0.5\text{ \AA}^2$ and $d=70.0\pm 0.5\text{ \AA}$ for the area per lipid and lamellar spacing, respectively.⁴ These dimensions are associated with a simulation cell of side box lengths L_x , L_y , and L_z with $A_{xy}\equiv\langle L_x\cdot L_y\rangle=1964.8\text{ \AA}^2$ and $\langle L_z\rangle=70.0\text{ \AA}$, where the x - y plane corresponds to the plane of the interface, the z axis is parallel to the membrane normal, and the brackets indicate that the average over time is taken. We used the Nosé–Hoover thermostat chain extended system isothermal-isobaric dynamics method, as implemented in the program PINY_MD.¹⁵ The utilization of a reversible multiple time step algorithm¹⁶ with a three-stage force decomposition (into intramolecular, short-range, and long-range intermolecular interactions) permitted the use of a time step of 5 fs.

The molecular and potential model used for the lipid molecules was the recent version of the CHARMM all-atom force field for lipids (CHARMM27).¹⁷ We used a rigid TIP3P model¹⁸ for the water molecules, which is consistent with the force field chosen for the lipids. All the motions involving hydrogen atoms were frozen and the constraints were handled by means of the SHAKE/ROLL and RATTLE/ROLL methods.¹⁶ The intermolecular parts of the force fields are pairwise additive functions, which consist of simple Lennard-Jones plus Coulomb terms, while the intramolecular interactions consisted of bonded potentials (bond stretching, bond bending, torsional motions) and nonbonded potentials (Lennard-Jones and electrostatic interactions for atoms separated by more than two bonds).

To overcome the boundary effects due to the finite size of the system, we used periodic boundary conditions. The short-range forces were computed using a cutoff of about 10 \AA and the minimum image convention, and the long-range

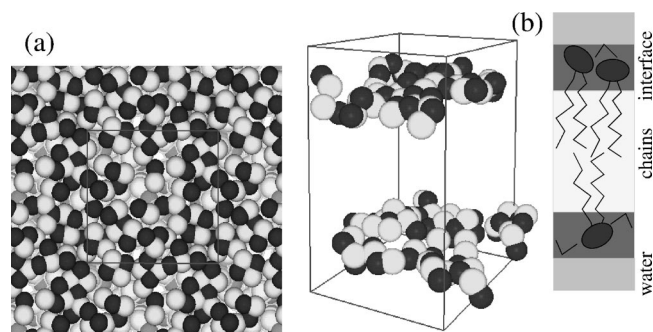


FIG. 2. Instantaneous configuration showing the arrangement of the phosphorus (light grey) and nitrogen (black) atoms of the lipid headgroups (a) at the plane of the lipid-water interface (top view of one of the leaflets) and (b) perpendicular to it (side view of the lipid bilayer membrane). For the sake of clarity, the water molecules are not displayed. The atoms are drawn as spheres with twice the van der Waals radii of the different species (phosphorus: $2 \times 3.8 \text{ \AA}$; nitrogen: $2 \times 3.3 \text{ \AA}$) and only those atoms located in the central orthorhombic simulation cell (colored light grey, with instantaneous side box lengths of $L_x = 46.5 \text{ \AA}$, $L_y = 42.5 \text{ \AA}$, and $L_z = 69.7 \text{ \AA}$) are shown in (b). Note that the simulation cell contains a single lipid bilayer membrane patch with periodic boundary conditions. The positions of the lipid hydrocarbon chains and the lipid-water interfaces of the two leaflets of the lipid bilayer membrane (where the water molecules are represented by their two covalent bonds), and the position of the bulk water are schematically indicated in (b, right).

forces were taken into account by means of the Particle Mesh Ewald method.¹⁹

III. RESULTS AND DISCUSSION

The experimental finding that in the L_α phase the lipid headgroups lie, on average, almost parallel to the membrane interface has been confirmed at the molecular level by classical MD simulations. However, the simulated systems were model membranes constituted usually by PCs with two saturated alkyl chains. In those systems, the main transition temperature, T_m , is quite high (room temperature or higher). Thus, in order to probe the L_α phase, the temperature range investigated was $\sim 50^\circ\text{C}$. In those conditions, the calculations using a variety of force fields and initial conditions revealed that the orientation of the lipid headgroup dipoles with respect to the bilayer normal followed an almost uniform distribution with a mean of $\sim 70^\circ$.^{5,20,21}

In the crystalline phase, the existence of two different headgroup conformations is common for PCs, PEs, and PGs.²² For instance, in the monoclinic form of dimyristoylphosphatidylcholine (DMPC), which crystallizes with two water molecules for each lipid, the two different molecules in the unit cell present headgroup dipole orientations of 17° and 27° with respect to the bilayer plane (63° and 73° with the bilayer normal, with a mean of 68°). This reflects two different kinds of interactions with the water molecules in the hydration shell and the neighboring lipid molecules.²² However, little is known about the organization of headgroup dipoles in this disordered and biologically relevant L_α phase at temperatures of experimental and biological interest.

The typical arrangement of the lipid headgroup dipole moments at room temperature is displayed in Figs. 2(a) and 2(b) for the SDPC lipid bilayer. For the sake of clarity, only

the phosphorus, P (light grey), and the nitrogen, N (black), atoms of the headgroups are drawn. The positions of the P and N atoms at the plane of the lipid-water interface and perpendicular to it are shown in Figs. 2(a) and 2(b), respectively, for an instantaneous configuration of the simulated system. In Fig. 2(b), right, a cartoon of the model membrane indicates the position the lipid hydrocarbon chains, the region of bulk water, and the position of the two interfaces where the lipid headgroups and the oxygen atoms of the carbonyl groups are hydrated by the water molecules. It is worth emphasizing that, in the present model, there is a positive net charge of $\sim 1e$ around the N atom (N^+) and a negative net charge of $\sim 1e$ around the P atom (P^-) of the lipid headgroup. The inhomogeneity of the system and the spatial organization of the P^- and N^+ oppositely charged atomic groups in (inter- and intramolecular) pairs with well defined separations is clearly illustrated in Fig. 2(a). On average, there are 2.4 intermolecular charge pairs (CP) per lipid molecule. Here, we have considered that there is a CP between two lipid molecules if the $N \cdots P$ distance between one of the P and one of the N atoms of the two molecules is smaller than R_{PN}^C . We chose R_{PN}^C to be the first minimum of the $g_{PN}(r)$ radial distribution function,⁴ which leads to $R_{PN}^C = 6.2 \text{ \AA}$. The picture that emerges from Fig. 2(a) is, however, rather complex and there is a rich variety of environments for the headgroup N^+ and P^- groups: from isolated molecules or pairs of molecules interacting simultaneously with each other via $P \cdots N$ and $N \cdots P$ pairs (double-pairs), to clusters of different sizes with molecules participating in multiple CPs. The quantitative evaluation of the different environments of the individual lipids through the calculation of the percentage of lipid molecules participating in n ($n = 0, 1, 2, 3, \dots$) CPs further supports this image at the studied conditions. Concretely, for the present SDPC lipid bilayer, we obtained the following values: 4% (0 CPs), 17% (1 CP), 31% (2 CPs), 30% (3 CPs), 13% (4 CPs), 3% (5 CPs), and 0% (≥ 6 CPs). Thus, we found that most of the molecules participate in either two or three CPs, but there is also a significant fraction of molecules participating in four CPs or in only one. We also observed a small fraction of isolated molecules and of molecules participating in as much as five CPs. It is worth noting that similar results were obtained for a DMPC lipid bilayer at similar conditions.²³ The $P-N \cdots P$ interactions are nonlinear and the $\angle N-P \cdots P$ angle distribution has a rather broad maximum at 43° . $P-N \cdots P$ interactions have been shown to occur directly or through a water molecule simultaneously bonded to both molecules.⁴ For the former, the peak becomes quite narrow and shifts to lower angles (40°) indicating a quite well defined arrangement of the $P-N \cdots P$ atoms, while it considerably broadens and is located at larger angles (48°) for the latter.

It is evident from Fig. 2(b) and simulations⁴ that, on average, the P^- atoms are located closer to the membrane interior than the N^+ atoms. To quantitatively evaluate this organization, we investigated the orientation of the headgroup dipole moment (basically, the $P \rightarrow N$ vector, denoted by $P-N$) of the lipid with respect to the membrane normal. In Fig. 3, we display the distribution of angles ϕ , $P(\phi)$, between the lipid headgroup $P-N$ vectors and the bilayer

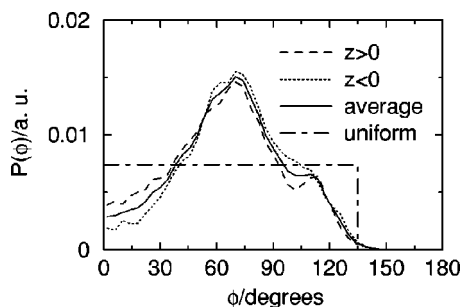


FIG. 3. Distribution of the ϕ angle between the headgroup P–N vector and the bilayer normal for each of the two different monolayers (denoted by $z > 0$ and $z < 0$) and the average value for the whole model membrane. The results are compared with a uniform distribution between 0° and 135° . The $P(\phi)$ curves are in arbitrary units.

normal, \hat{n} . The headgroup dipoles at room temperature present a preferential orientation along the plane of the interface. Specifically, we obtained that the mean orientations with respect to the bilayer normal of the P–N vector, the headgroup dipole ($\hat{\mu}_H$), and the total lipid dipole are 69° , 74° , and 80° , respectively. Furthermore, these values also correspond to the most probable orientations. This considerably reduces the component of the dipole moment perpendicular to the bilayer plane from $\langle \mu_0^H \rangle = 16.76$ D (for the total headgroup dipole moment) to $\langle \mu_z^H \rangle = 4.21$ D (for the direction parallel to the membrane normal, z axis). The discrepancies between the results obtained for the two different monolayers indicate the likely magnitude of the statistical errors present in the simulations.

The deviations of the present P–N angle distribution at 30°C from the uniform distribution obtained at higher temperatures from MD simulations^{5,20,21} are evidenced in Fig. 3. Our results are consistent with other calculations using a diversity of force fields and initial conditions at similar temperatures for systems with a low T_m temperature.^{24–27} This indicates a qualitatively different behavior in the L_α phase upon cooling. The P→N (or, equivalently, $\hat{\mu}_H$) orientation with respect to the bilayer normal (at least in PCs) thus changes from an almost uniform distribution at high temperatures ($\sim 50^\circ\text{C}$) to a distribution with a most probable orientation of about 70° , i.e., 20° above the bilayer plane, pointing toward the water region. Note that the mean orientation is quite similar in both situations and this value is, in turn, in excellent agreement with experiment. Its microscopic origin is, however, different in each case. At higher temperatures, the P–N orientation is basically limited by geometrical constraints, namely, the hindered motion of the headgroups caused by the presence of the hydrophobic lipid acyl chains. At lower temperatures, it is due to a prevalent orientation of the headgroup dipoles with respect to the membrane surface. For the present lipid bilayer, we found also a symmetric maximum, though with a lower population, at 110° , i.e., 20° underneath the bilayer plane, pointing toward the bilayer interior.

The roughness of the interface is clearly illustrated in Fig. 4, where the evolution of the angle ϕ with time is shown for a set of representative molecules. Our results indicate that molecules with preferential headgroup orientations of $\pm 20^\circ$

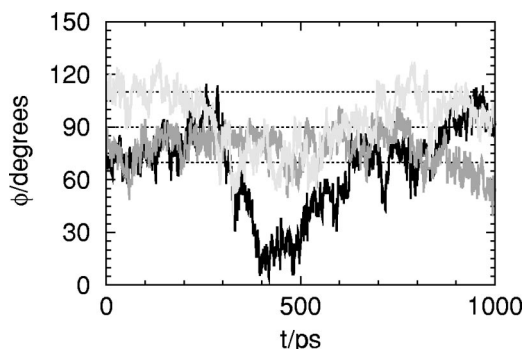


FIG. 4. Temporal evolution of the angle ϕ between the P–N vector and the bilayer normal for a representative set of lipid molecules: molecule 1 (light grey line), molecule 2 (black line), and molecule 3 (dark grey line). The three curves represent three different characteristic behaviors of the lipid headgroup dipoles (see text). The angles corresponding to the positions of the maxima of the $P(\phi)$ function ($\phi = 70^\circ$ and $\phi = 110^\circ$) and the value corresponding to the x - y projection of the plane of the interface ($\phi = 90^\circ$) are indicated by dotted lines.

with respect to the membrane plane are quite stable, although transitions between both states take place in the nanosecond time scale investigated (light grey and dark grey curves). The rest of the molecules are remarkably free (black curve). This behavior agrees with what occurs in more ordered lamellar phases. For instance, in the gel-phase ($L_{\beta'}$), from MD simulations it was shown that the P–N orientation displays a bimodal distribution.²⁸ In those calculations, the authors found two roughly equal populations at 41° and 84° with the bilayer normal, pointing toward the water phase, for dipalmitoylphosphatidylcholine (DPPC) at 19°C . This indicates two dominant configurations of the lipid headgroups with a mean value of 70° . This bimodal distribution is reminiscent of the structure of the crystal. It is clear from the present study that there is a different behavior with temperature. These two different regimes of the lipid headgroups, one with preferential orientation (order) and the other with uniform orientation (disorder) are present in the fluid lamellar phase, L_α .

The preferential orientation of the headgroup dipoles has the expected counteracting effect on the water molecules, which are polarized at the lipid-water interface. This influence is shown in Fig. 5(a), where the mean value of the cosine of the angle, θ , of the water dipole moment with respect to the bilayer normal is plotted as a function of the position of the centers of mass of the water molecules along the z axis. Note that the water density profiles do not penetrate deeper than the position of the density distributions of the glycerol backbone,⁴ which is indicated here by the lack of data in the region close to the bilayer center ($z = 0 \text{ \AA}$). The water dipoles are oriented pointing toward the bilayer interior for those molecules close to the water-lipid interface (indicated by the negative values of $\langle \cos(\theta) \rangle$). The situation is the opposite for those molecules located deeper in the interfacial region. There, the water molecules align their dipole moments pointing toward the water bulk region.

The organization at the interface of water and lipid molecular dipoles affects the charge distribution in the direction of the membrane normal and, consequently, the electrostatic potential across the interface (membrane potential). The elec-

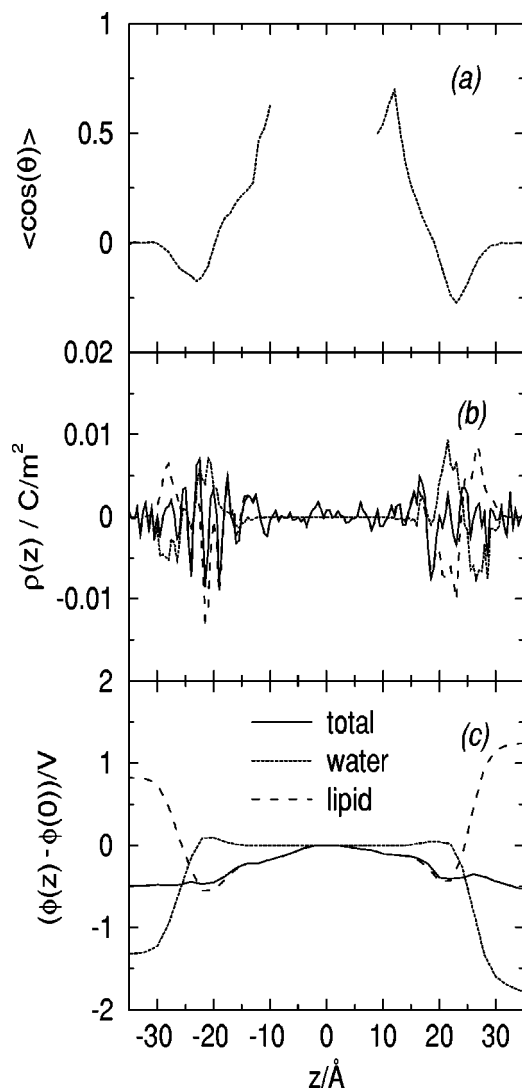


FIG. 5. (a) Mean value of the cosine of the angle θ between the molecular dipole moment of the water molecules and the bilayer normal as a function of the position of the molecular centers of mass along z . Charge density (b) and electrostatic potential (c) profiles. The contributions from the water (dotted lines) and lipid (dashed lines) molecules are shown explicitly. The bilayer center is located at $z=0$ \AA .

trostatic potential profile, $\phi(z)$, can be estimated using Poisson's equation, which reads: $-\nabla^2 \phi(z) = (1/\epsilon_0)\rho(z)$, with $\rho(z)$ being the charge density as a function of z . Thereby, the electrostatic potential across the membrane is given by: $\phi(z) - \phi(0) = -(1/\epsilon_0) \int_0^z \int_0^{z'} \rho(z'') dz'' dz'$, where $\phi(0)$ is the electrostatic potential at the bilayer center. In Figs. 5(b) and 5(c), the charge distribution and the electrostatic potential are plotted as a function of z . To investigate the origin of the different features of the curves, we calculated the contributions due to the lipid and the water molecules, which are plotted separately in Fig. 5. The lipid dipoles are oriented in such a way that create a negative potential in the membrane interior. The water molecules excessively cancel this effect by creating a positive potential in the bilayer core. These two large counteracting contributions lead to a considerable positive potential in the interior of the bilayer. In the present calculations, we found $\phi(z) - \phi(0) \approx -500$ mV, which is in agreement with the available experimental data.³ From the

center of the bilayer toward the interface, the $\phi(z)$ curves obtained for the lipids indicate a charge distribution with the following characteristics: a zone with a weak positive charge (located around the carbonyl position), a region of negative charge corresponding to the position of the negative charged phosphate groups, and a positive region at the interface corresponding to the position of the positively charged choline groups (N^+). This is shown in Fig. 5(b), where we plot the results obtained for the charge distributions of the different molecules and the whole system. The charge distribution for water shows an opposite picture. From the interior toward the region of bulk water, one crosses a region of a very weak negative charge density, a positive charge, and a negative charge densities located at similar positions as those for the lipid but with reversed signs. The role of the water molecules is clearly seen as overcompensating the charge distribution created by the lipid dipoles through the water polarization, which here should be understood as preferential orientation.

The existence of a symmetric orientation of the head-group dipole, pointing toward the membrane interior, opens the possibility of reversing the charge density of the lipids and, consequently, of the water molecules. The inversion of the lipid dipole orientation may be differently cancelled by water because of the presence of the hydrophobic lipid bilayer interior. In similar situations, the membrane potential of model membranes has been found to have the opposite sign.²⁹ The reversed orientation of the headgroup dipoles may be achieved, for instance, via the incorporation of external elements into the pure neutral membrane. The modification of the electrostatic interactions among the phospholipid headgroups in each monolayer could not only modify the membrane permeability to small solutes and/or water or facilitate the insertion of membrane peptides and/or proteins but may also affect protein function directly, via lipid-protein interactions, or indirectly, for instance, by changing the bilayer curvature stress³⁰ or by changing the lateral pressure profile.³¹

IV. CONCLUSIONS

We have investigated the electrostatic properties at the lipid-water interface of a model neutral membrane by performing an atomistic molecular dynamics simulation study in the fluid lamellar phase, L_α , at room temperature and ambient pressure. We considered a fully hydrated 1-stearoyl-2-docosahexaenoyl-*sn*-glycero-3-phosphocholine lipid bilayer because it has a low main phase transition temperature. The results obtained are in good agreement with the available experimental data. We found that the lipid headgroups are organized at the interface in intermolecular and intramolecular charge pairs between the oppositely charged choline (N^+) and phosphate (P^-) groups, with molecules participating in an average number of 2.4 intermolecular pairs. The local spatial distribution of positive and negative groups is, however, inhomogeneous and we observed a rich variety of environments for the N^+ and P^- groups, with lipid headgroups participating in different numbers of those charge pairs.

Our analysis has shown that the orientation of lipid $\text{P} \rightarrow \text{N}$ vectors (basically the lipid headgroup dipole moments)

with respect to the direction normal to the membrane surface does not follow, at room temperature, a uniform distribution. Instead, headgroup dipoles are most probably oriented forming an angle of approximately 70° , pointing toward the water region. The comparison with other computations at similar conditions^{24–27} indicates that the results obtained in the present work do not depend on the particular details of the model. This preferential orientation of the lipid dipole moments is, however, qualitatively different from previous results obtained at higher temperatures^{5,20,21} in the fluid lamellar phase, which suggests a different behavior upon cooling. At high temperatures, there is a regime where the lipid headgroup dipoles are uniformly distributed with orientations spanning 0° – 135° with respect to the bilayer normal,^{5,20,21} whereas, around room temperature, they mostly lie almost parallel to the interface. Even though both situations lead to similar mean orientations ($\approx 70^\circ$), which is in excellent agreement with experiment, the origin is different in each case.

For the present system, we also found a symmetric orientation of the headgroup dipoles (at 110°), pointing towards the interior of the membrane, and the temporal evolution of the lipid dipole orientation indicated that transitions between the two different states take place in the nanosecond time scale studied. Despite the differences observed from simulations for the P→N orientations in the fluid lamellar phase at different conditions, the water molecules are polarized at the interface in a similar way, creating a positive potential in the bilayer interior and excessively counteracting the negative potential created by the lipid molecules, giving rise to a considerable positive potential, in agreement with experiment.

Our results have revealed the presence of both ordered and disordered lipid headgroup dipoles in the (disordered) fluid lamellar phase of model membranes. They also provide further insights into the molecular origin of the structure and dynamics of the membrane interface in more realistic model membranes at temperatures of biological and experimental interest and, specially, the electrostatic properties, which play a fundamental role in the interactions among membranes or vesicles, membranes and biological molecules, and membranes with external fields.

ACKNOWLEDGMENTS

This work has been supported by the National Institutes of Health through Grant No. GM 40712. The calculations were performed on the Origin2000 at the National Center for Supercomputing Applications (NCSA). We gratefully acknowledge stimulating discussions with Myer Bloom and with Klaus Gawrisch.

- ¹R. Lipowsky and E. Sackmann, Eds., *Structure and Dynamics of Membranes*, in *Handbook of Biological Physics*, Vol. 1 (Elsevier, Amsterdam, 1995).
- ²W. M. Gelbart, R. F. Bruinsma, P. A. Pincus, and V. A. Parsegian, *Phys. Today* **53**, 38 (2000).
- ³K. Gawrisch, D. Ruston, J. Zimmernberg, V. A. Parsegian, R. P. Rand, and N. Fuller, *Biophys. J.* **61**, 1213 (1992).
- ⁴L. Saiz and M. L. Klein, *Biophys. J.* **81**, 204 (2001).
- ⁵M. Pasenkiewicz-Gierula, Y. Takaoka, H. Miyagawa, K. Kitamura, and A. Kusumi, *Biophys. J.* **76**, 1228 (1999).
- ⁶J. Seelig, P. M. Macdonald, and P. G. Scherer, *Biochemistry* **26**, 7535 (1987).
- ⁷P. G. Scherer and J. Seelig, *Biochemistry* **28**, 7720 (1989); H. U. Gally, W. Niederberger, and J. Seelig, *ibid.* **14**, 3647 (1975); H. Akutsu and T. Nagamori, *ibid.* **30**, 4510 (1991).
- ⁸J. A. Barry, T. P. Trouard, A. Salmon, and M. F. Brown, *Biochemistry* **30**, 8386 (1991).
- ⁹J. Hamilton, R. Greiner, N. Salem, and H. Y. Kim, *Lipids* **35**, 863 (2000), and references therein.
- ¹⁰L. Saiz and M. L. Klein, *J. Am. Chem. Soc.* **123**, 7381 (2001).
- ¹¹B. J. Litman and D. C. Mitchell, *Lipids* **31**, s193 (1996).
- ¹²M. F. Brown, *Chem. Phys. Lipids* **73**, 159 (1994).
- ¹³M. Bloom, *Biol. Skr. Dan. Vid. Selsk.* **49**, 13 (1998).
- ¹⁴K. Palczewski, T. Kumasaka, T. Hori *et al.*, *Science* **289**, 739 (2000).
- ¹⁵M. E. Tuckerman, D. A. Yarne, S. O. Samuelson, A. L. Hughes, and G. J. Martyna, *Comput. Phys. Commun.* **128**, 333 (2000).
- ¹⁶G. J. Martyna, M. E. Tuckerman, D. J. Tobias, and M. L. Klein, *Mol. Phys.* **87**, 1117 (1996).
- ¹⁷M. Schlenkrich, J. Brickmann, A. D. MacKerell, Jr., and M. Karplus, in *Biological Membranes: A Molecular Perspective from Computation and Experiment*, edited by K. M. Merz and B. Roux (Birkhauser, Boston, 1996); S. E. Feller and A. D. MacKerell, Jr., *J. Phys. Chem. B* **104**, 7510 (2000).
- ¹⁸W. L. Jorgensen, J. Chandrasekhar, J. D. Madura, R. W. Impey, and M. L. Klein, *J. Chem. Phys.* **79**, 926 (1983).
- ¹⁹D. Frenkel and B. Smit, *Understanding Molecular Simulation* (Academic, London, 1996).
- ²⁰K. C. Tu, D. J. Tobias, and M. L. Klein, *Biophys. J.* **69**, 2558 (1995).
- ²¹U. Essmann and M. L. Berkowitz, *Biophys. J.* **76**, 2081 (1999).
- ²²D. M. Small, *The Physical Chemistry of Lipids: From Alkanes to Phospholipids*, in *Handbook of Lipid Research*, Vol. 4 (Plenum, New York, 1986).
- ²³L. Saiz, S. Bandyopadhyay, and M. L. Klein, preprint (2001).
- ²⁴M. T. Hyvönen, T. T. Rantala, and M. Ala-Korpela, *Biophys. J.* **73**, 2907 (1997).
- ²⁵T. Husslein, D. M. News, P. C. Pattnaik, Q. F. Zhong, P. B. Moore, and M. L. Klein, *J. Chem. Phys.* **109**, 2826 (1998).
- ²⁶S. Bandyopadhyay, J. C. Shelley, and M. L. Klein, *J. Phys. Chem. B* **105**, 5979 (2001).
- ²⁷In previous computer simulations at room temperature in the fluid lamellar phase (Refs. 24 and 25), the $P(\phi)$ distributions were normalized in such a way that a uniform distribution of the headgroup dipoles in a (three-dimensional) sphere corresponds to a $\sin(\phi)$ function. Consequently, this is the first work (and later also in Ref. 26) where the $P(\phi)$ distribution is properly normalized at room temperature, so the deviations from the almost uniform distribution observed at higher temperatures are evident.
- ²⁸K. C. Tu, D. J. Tobias, J. K. Blasie, and M. L. Klein, *Biophys. J.* **70**, 595 (1996).
- ²⁹A. M. Smondyrev and M. L. Berkowitz, *Biophys. J.* **76**, 2472 (1999).
- ³⁰J. A. Lundæ, A. M. Maer, and O. S. Andersen, *Biochemistry* **36**, 5695 (1997); J. A. Lundæ, P. Birn, J. Girshman, A. J. Hansen, and O. S. Andersen, *ibid.* **35**, 3825 (1996).
- ³¹R. S. Cantor, *J. Phys. Chem. B* **101**, 1723 (1997).